



Cite this: DOI: 10.1039/d5ob01686j

Received 26th October 2025,  
Accepted 23rd December 2025

DOI: 10.1039/d5ob01686j  
rsc.li/obc

## Recent advances in Pd-catalysed decarboxylative asymmetric allylic alkylation

Niamh Lehane and Patrick J. Guiry \*

This comprehensive review on the Pd-catalysed decarboxylative asymmetric allylic alkylation details the development of this important transformation from its origins to more recent advances. Selected examples of this synthetically mild methodology being applied in natural product synthesis are given. The mechanism is explored in detail, to provide a thorough insight on the current understanding, which is built upon the combination of experimental and computational studies.

### Introduction

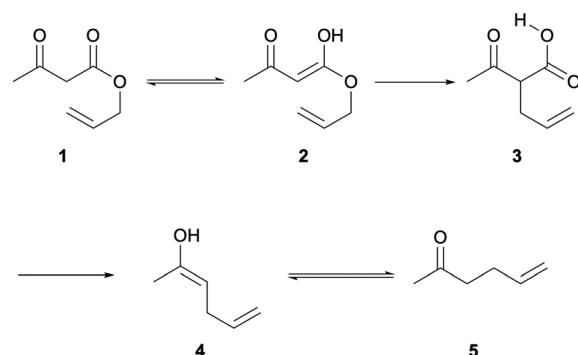
In 1940, Carroll reported a variant of the ester Claisen rearrangement which involved heating acyclic acetoacetate **1** in the presence of a base, inducing a [3,3]-sigmatropic rearrangement and decarboxylation to give  $\gamma,\delta$ -unsaturated ketone **5** (Scheme 1).<sup>1</sup> This was the first report of insertion of an allylic group  $\alpha$ - to a carbonyl but the reaction however has found little applicability in organic synthesis due to the harsh reaction conditions required to induce reactivity (temperatures of between 130–220 °C).<sup>2</sup> Though it did find use in the industrial synthesis of terpenes by BASF.<sup>3</sup>

The Tsuji–Trost reaction is a milder synthetic route for the formation of allylic compounds, proceeding *via* Pd- $\pi$ -allyl complexes. Coordination of the Pd<sup>0</sup> catalyst to the allyl-containing compound **6** followed by oxidative addition generates Pd- $\pi$ -allyl complex **7** which is then attacked by an activated nucleophile such as an enolate, amine or alcohol to result in an allylic substitution product **8** (Scheme 2).

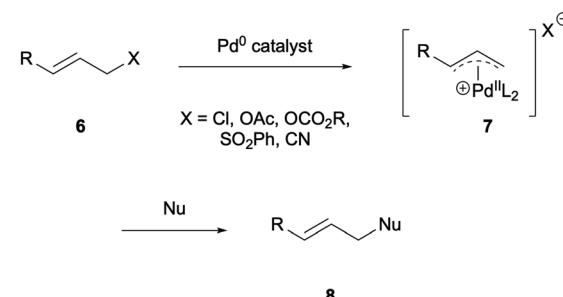
In 1965, Tsuji reported the reaction of  $\pi$ -allylpalladium chloride with nucleophiles such as ethyl malonate and acetoacetate to yield racemic monoallylated and diallylated species.<sup>4</sup> This work was further developed by Trost in 1973, who described catalytic monoalkylation of alkyl substituted  $\pi$ -allylpalladium complexes with phosphane ligands.<sup>5</sup> In 1977 Trost reported the first asymmetric allylic alkylation (AAA) with enantioselectivities of up to 24% ee.<sup>6</sup> In 1980 Saegusa and Tsuji independently reported the synthesis of  $\alpha$ -allylic ketones *via* a Pd-catalysed route, or decarboxylative allylation, of  $\beta$ -keto allyl esters **9** (Scheme 3).<sup>7,8</sup> In this reaction both the nucleophile and electrophile are generated *in situ* from the allyl ester, which adds to its synthetic use, as the need for pre-formed enolates is eliminated.

### Development of the Pd-catalysed DAAA

The first decarboxylative asymmetric allylic alkylation (DAAA) of  $\beta$ -keto allyl esters, yielding acyclic  $\alpha$ -allyl ketones was reported by Tunge 20 years later, in 2004. His system employed the chiral DACH-phenyl Trost ligand **L1** to access products **12** with excellent enantioselectivities, of up to 99% ee (Scheme 4).<sup>9</sup> The substrate scope however was quite limited,

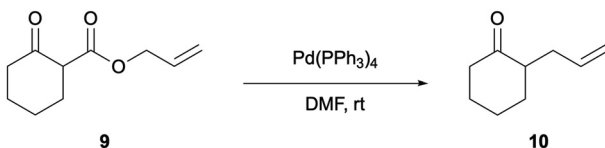


Scheme 1 The Carroll rearrangement of  $\beta$ -keto allyl esters.

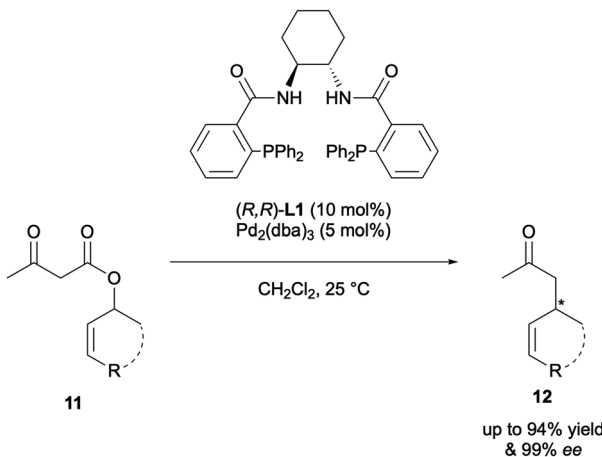


Scheme 2 General scheme of Tsuji–Trost allylation.





Scheme 3 Decarboxylative allylation by Saegusa.

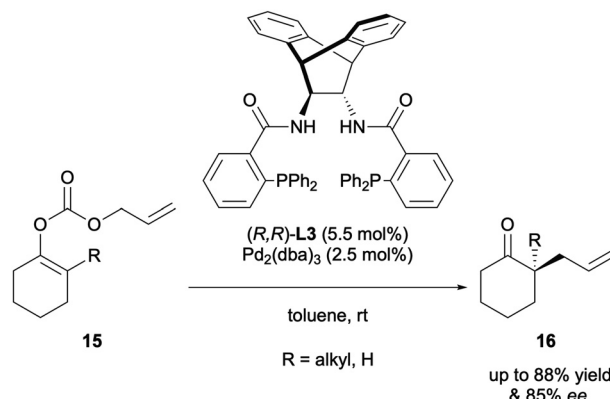


Scheme 4 First reported DAAA by Tunge.

with only eight examples and just one of those substrates was cyclic.

The same year, Stoltz reported the formation of cyclic  $\alpha$ -allyl ketones *via* DAAA using allyl enol carbonate substrates 13 (Scheme 5).<sup>10</sup> Ligand screening showed that the chelating P,N ligand, *tert*-butyl-phosphinoxazoline ((*S*)-*t*-BuPHOX) L2, was the most effective, affording a 89% ee. Access to these 2-allyl-2-alkyliclohexanones compounds had previously not been possible *via* AAA due to the enolate scrambling *in situ*.

Trost published a similar system in 2005, employing the same allyl enol carbonate substrates to carry out the enantioselective allylic alkylation of cyclic ketones (Scheme 6). A ligand screen revealed that his own P,P ligand (*R,R*)-ANDEN-phenyl Trost L3 afforded the highest yields and levels of asym-

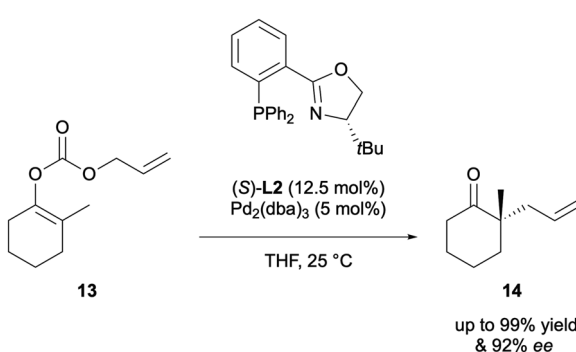


Scheme 6 DAAA of allyl enol carbonates by Trost.

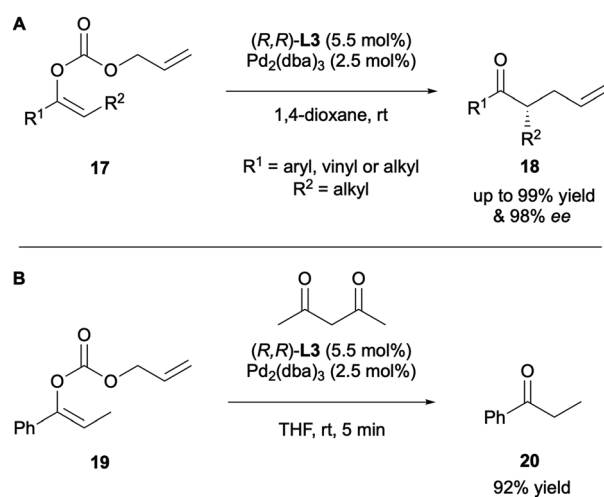
metric inductions.<sup>11</sup> This report also included the generation of tertiary  $\alpha$ -allyl stereocentres in up to >99% ee.

These results conflict with the earlier reports by Stoltz, who observed that P,P ligands screened gave poor to moderate enantioselectivities. As both systems used allyl enol carbonates as substrates, it was suggested that there were two different mechanisms (inner sphere *vs.* outer sphere, *vide infra*) occurring for each ligand.

Trost and co-workers extended the substrate scope of their DAAA protocol to include acyclic ketones 18 (Scheme 7A).<sup>12</sup> Several key observations were made in this work. The dialylated species was isolated when toluene and THF were employed as solvents, which was overcome by running the reactions in 1,4-dioxane. It was discovered that the degree of substituent branching and the *E/Z* configuration of the starting material effected the rate and enantioselectivity of the reaction significantly. The *E*-isomer supported higher levels of asymmetric induction in a much shorter reaction time compared to the *Z*-isomer. However, the *E/Z* configuration did not affect the regioselectivity. The electronic nature of the  $\text{R}_1$  sub-



Scheme 5 DAAA of allyl enol carbonates by Stoltz.



Scheme 7 DAAA of acyclic ketones by Trost.

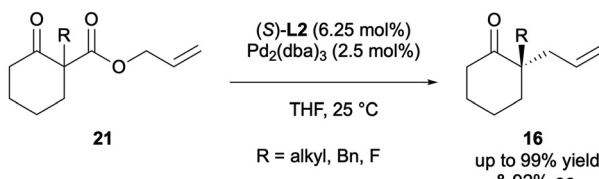


stituent did influence the levels of enantioselectivity, with electron-withdrawing groups, such as a pyridyl substituent, giving a decrease in enantioselectivity from 98% ( $R_1 = 2\text{-MeOC}_6\text{H}_4$ ) to 73% ee. All these results imply that there is both a steric and an electronic element in the asymmetric induction of the DAAA reaction. Finally, as they had observed the formation of a tertiary centre, a proton source was introduced to the reaction and different sources were screened. Protonated product **20** could be accessed in up to 92% yield, with acetylacetone proving to be the optimal proton source (Scheme 7B).

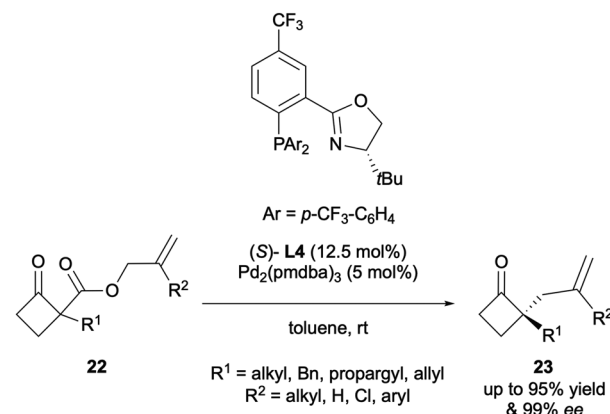
Although allyl enol carbonates have proven to be desirable substrates for DAAA, giving rise to high yields and ees, they have limitations. Issues arise with both their stability and regioselective synthesis, which places a limit on the synthetic use of this methodology. To overcome this concern, Stoltz built upon the earlier work of Saegusa and Tsuji, and their use of  $\beta$ -keto-allyl esters as substrates. These compounds are bench stable, easily prepared, and were found to be excellent substrates for DAAA (Scheme 8).<sup>13</sup> The employment of  $\beta$ -oxoesters in this methodology is an example of '*stereoab ablative enantioconvergent catalysis*'. The chiral centre within the substrate collapses and is then reformed to yield the enantio-enriched product.

## Recent advances in the Pd-catalysed DAAA

Since it was first reported, the DAAA reaction has been significantly developed, especially with respect to expanding the substrate scope. The topic has been reviewed on several occasions since 2004<sup>14,15</sup> and this article aims to provide an update on the most recent developments. Most reports of the reaction employ the original high-performing ligands: the PHOX-type or Trost-type ligands. Initial studies explored larger cyclic ketone systems, such as cyclohexanones, cycloheptanones and cyclooctanones,<sup>10,13</sup> although Stoltz reported the DAAA of cyclobutanones in 2013 (Scheme 9).<sup>16</sup> It was found that the electron-deficient (*S*)-(CF<sub>3</sub>)<sub>3</sub>-*t*-Bu-PHOX ligand **L4** with Pd<sub>2</sub>(pmdba)<sub>3</sub> (pmdba = 4,4'-dimethoxydibenzylideneacetone) generated the best levels of asymmetric induction, enabling access to products **23** in up to 99% ee. A variety of  $\alpha$ -alkyl substituents were well tolerated under the catalytic system and substitution on the allyl fragment was also supported. The synthetic utility of these cyclobutanone DAAA products was exemplified by further transforming them to lactams, lactones,



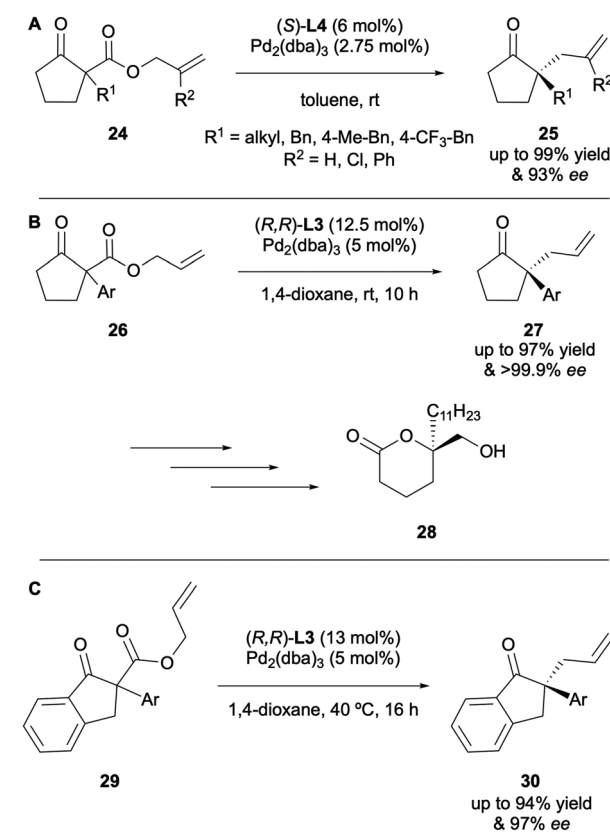
Scheme 8 DAAA of  $\beta$ -keto allyl esters by Stoltz.



Scheme 9 DAAA of cyclobutanones by Stoltz.

cyclopentanones and spirocyclic cyclobutanes, all of which involved retention of the high ees installed by the DAAA reaction.

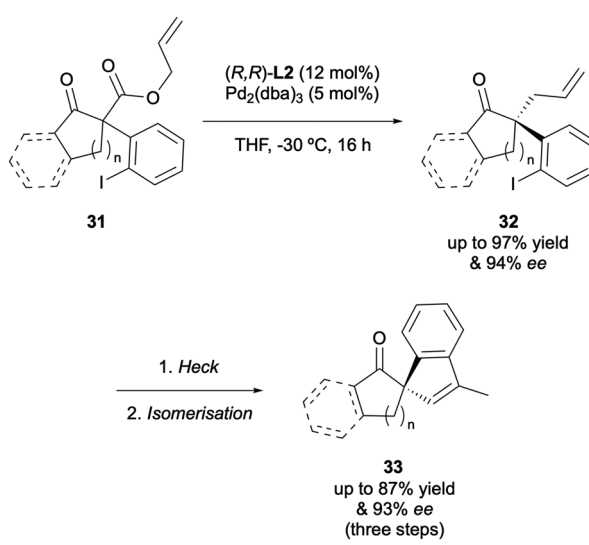
Subjecting cyclopentanones to the DAAA protocol proved to be a challenge due to poor yields and levels of stereoinduction until 2015, when Stoltz and co-workers published the synthesis of  $\alpha$ -allyl- $\alpha$ -benzyl cyclopentanones with enantioselectivities of up to 99% ee (Scheme 10A).<sup>17</sup> The substrate scope study provided a key insight into how important substrate electronics



Scheme 10 DAAA of  $\alpha$ -alkyl/aryl cyclopentanones and  $\alpha$ -aryl indanones.

were. It was observed that full conversion to the electron-rich *p*-methoxybenzyl-cyclopentanone was achieved in 8 h but the electron-poor *p*-(CF<sub>3</sub>)-benzyl analogue produced a low yield of 56% even after 96 h. In 2016 Guiry reported the synthesis of  $\alpha$ -allyl- $\alpha$ -aryl cyclopentanones **24** *via* a highly enantioselective DAAA that employed (*R,R*)-ANDEN-phenyl Trost to generate unprecedented enantioselectivities, of up to >99.9% ee (Scheme 10B).<sup>18</sup> In many of the early substrate scopes, substituents present on the newly generated  $\alpha$ -stereocentre were typically restricted to small alkyl groups. This was the first example of a wide range of substrates bearing electron-rich mono- and di-*ortho*-substitution patterns on an aromatic group in the DAAA protocol. The advantage of this development was highlighted by its use in the synthesis of marine natural product (+)-tanikolide **28**, which possesses anti-fungal properties. More recently, Guiry and co-workers described the application of  $\alpha$ -aryl indanone substrates to DAAA under similar conditions to access highly enantioselective products **30** in up to 97% ee (Scheme 10C).<sup>19</sup> For both the reactions described in Scheme 10B and C, the optimal results were obtained for those substrates possessing aryl groups with di-*ortho*-substitution (2,4,6-trimethoxyphenyl, 2,6-dimethoxyphenyl) and naphthyl benzyl and methyl ethers. For both sets of substrates, strict matching of substrates and chiral Pd complexes was required.

In 2024 Christoffers and co-workers described an interesting tandem DAAA and Heck reaction in the synthesis of optically active spirocycles (Scheme 11).<sup>20</sup> The initial DAAA transformation of selected carbocycles proceeded smoothly to generate the intermediate products in high enantioselectivities of up to 94% ee. These were subsequently converted into spirocyclic structures *via* a Heck reaction and isomerisation to access the *endo*-products in quantitative yields and selectivities.



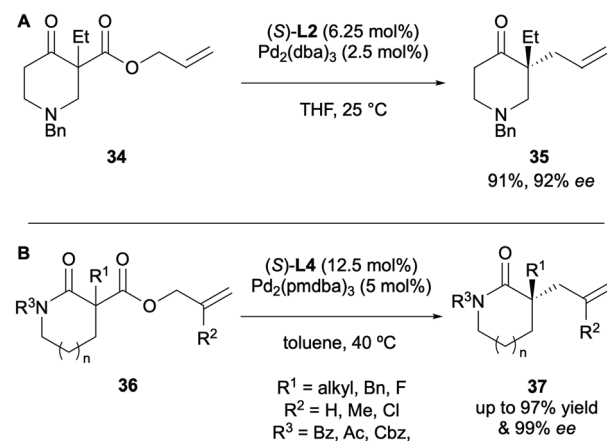
**Scheme 11** DAAA products as intermediates for spirocyclic structures by Christoffers.

The DAAA of heterocyclic compounds has also been well explored, due to these motifs being prevalent in natural products and compounds of biological interest.<sup>21</sup> Stoltz in particular has reported the enantioselective synthesis of a number of N-heterocyclic compounds since 2005. In one of his first reports on DAAA catalysis he demonstrated the applicability of the system with a 4-piperidone substrate **34**, with a 92% ee (Scheme 12A).<sup>13</sup> In 2012 his group published the synthesis of quaternary stereocentres in 5-, 6- and 7-membered lactams *via* DAAA (Scheme 12B).<sup>22</sup> It was discovered that electron-withdrawing nitrogen protecting groups were crucial for reactivity, with *N*-alkyl substrates being poor substrates for the catalysis. Once again, they found that electron-poor (*S*)-(CF<sub>3</sub>)<sub>3</sub>-*t*-Bu-PHOX **L4** was the superior ligand for the transformation and displayed high levels of asymmetric induction, with enantioselectivities of up to 99% ee being achieved.

In 2019 Stoltz further investigated lactams in the DAAA reaction and reported that (*R,R*)-ANDEN-phenyl Trost **L3** could generate highly enantioselective benzo-fused and non-benzo-fused lactams with ee values of up to 98% (Scheme 13A).<sup>23</sup> Most recently in 2024, Guiry demonstrated the synthesis of  $\alpha$ -allyl- $\alpha$ -aryl lactams in an enantioselective fashion *via* DAAA to access a range of products possessing highly sterically hindered quaternary stereocentres in high enantioselectivities of up to 82% ee (Scheme 13B).<sup>24</sup>

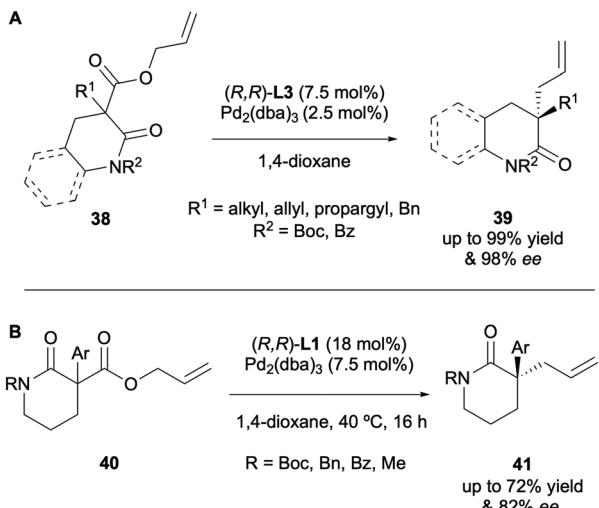
Taylor and co-workers described the DAAA of both  $\alpha$ -aryl and  $\alpha$ -alkyl oxindoles in 2011.<sup>25</sup> (*R,R*)-ANDEN-phenyl Trost **L3** was the optimal ligand and it was found that substrates displayed solvent dependency with varied results being obtained whether DME, THF or toluene were used (Scheme 14A). In 2017 Guiry and co-workers reported the DAAA of oxindoles with (*R,R*)-ANDEN-phenyl Trost **L3** again, to include a broader scope of  $\alpha$ -aryl substrates (Scheme 14B).<sup>26</sup>

A number of N,N-heterocycles have been applied to the DAAA methodology by Stoltz and co-workers. In 2015 the DAAA of *N*-4-benzylated piperazin-2-ones displayed excellent yields and enantioselectivities, of up to 98% and 99% ee, respectively (Scheme 15A).<sup>27</sup> The synthetic utility of this trans-

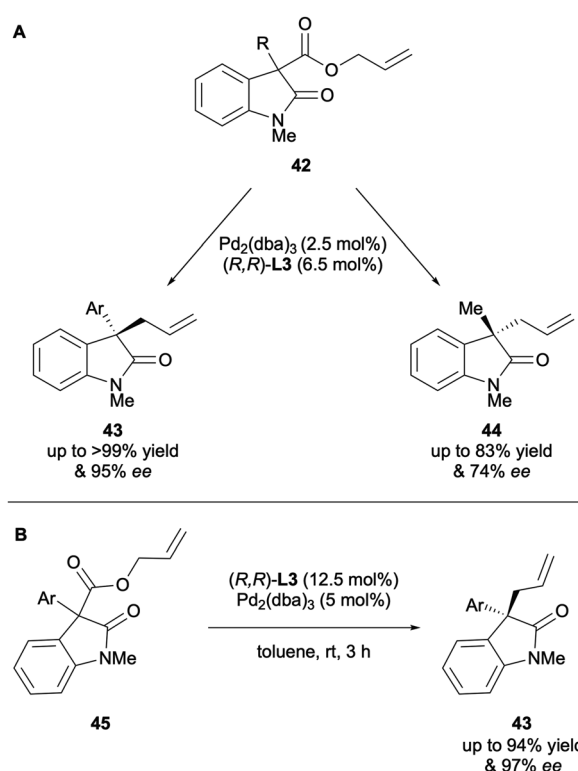


**Scheme 12** DAAA of lactams by Stoltz.



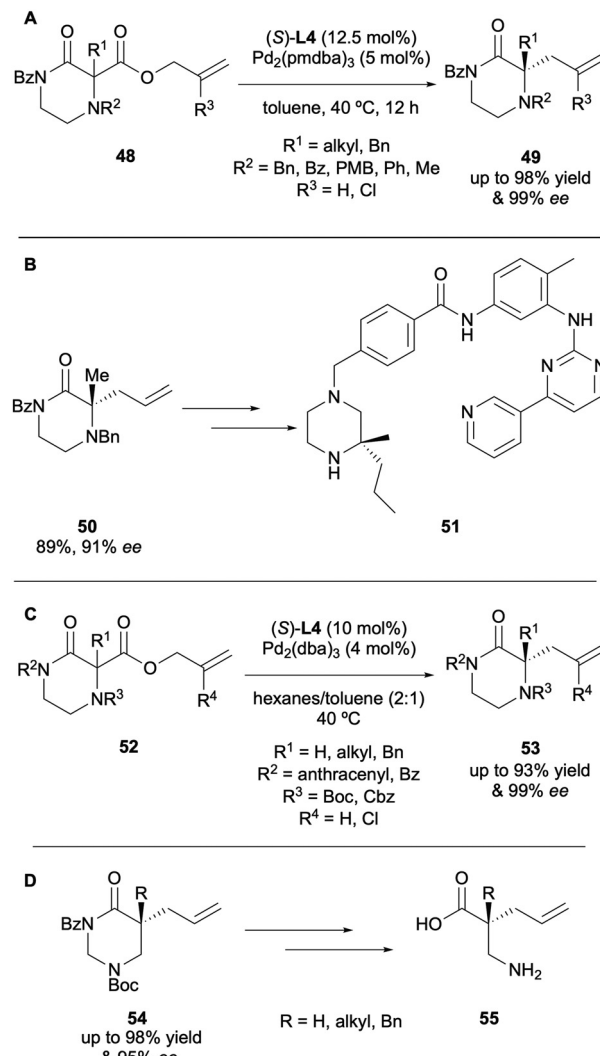


**Scheme 13** DAAA of lactams by Trost & Guiry



**Scheme 14** DAAA of oxindoles by Taylor & Guiry.

formation was exhibited by the use of **50** in the synthesis of an Imatinib analogue **51** (Scheme 15B). However, in attempting to use other substrates to synthesise medicinally relevant compounds two issues arose, relating to difficult substrate synthesis and chemoselectivity issues in further functionalisation, namely the PMB group proved impossible to cleave under conditions that were orthogonal to the allylic motif. These challenges were overcome in 2019 with the development of a more streamlined approach to substrate synthesis and installing a



**Scheme 15** DAAA of piperazin-2-ones by Stoltz

Boc protecting group at *N*-4, which is thought to reduce the nucleophilicity of this position compared to having a Bn group present (Scheme 15C).<sup>23</sup> The report also demonstrated the application of tetrahydropyrimidin-2-ones to the DAAA protocol, which provided access to the corresponding  $\beta^{2,2}$ -amino acids *via* hydrolysis (Scheme 15D).

In 2020 the Stoltz group reported the DAAA of  $\alpha$ -enaminones as a new class of substrate that performed very well, with yields of up to 99% and enantioselectivities of up to 99% ee with L2 and  $Pd_2(dmdba)_3$  ( $dmdba = 3,5,3',5'$ -dimethoxydibenzylideneacetone) (Scheme 16).<sup>28</sup> The highly enantioenriched products could serve as useful synthetic building blocks and in addition, it is believed that the  $\alpha$ -heteroatom could have a role in enantioselectivity enhancement *via* chelation. Their work on these N,N-heterocyclic motifs also includes cyclic imides,<sup>29</sup> 1,4-diazepan-5-ones,<sup>30</sup> and 4-imidazolidinones (Fig. 1).<sup>31</sup>

Shibasaki reported the DAAA of isoxazolidin-5-ones **61** in 2018, employing (*S,S*)-ANDEN phenyl Trost **L3** as the most effective ligand to achieve high enantioselectivities of up to

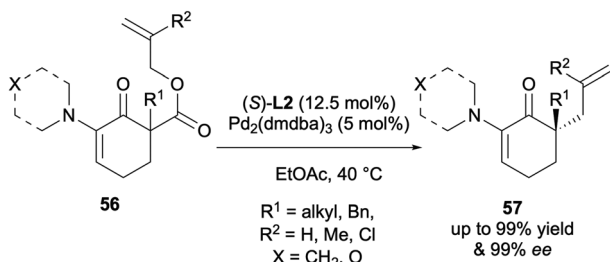
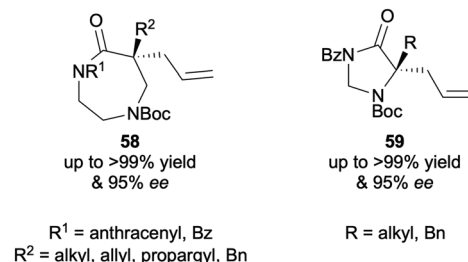
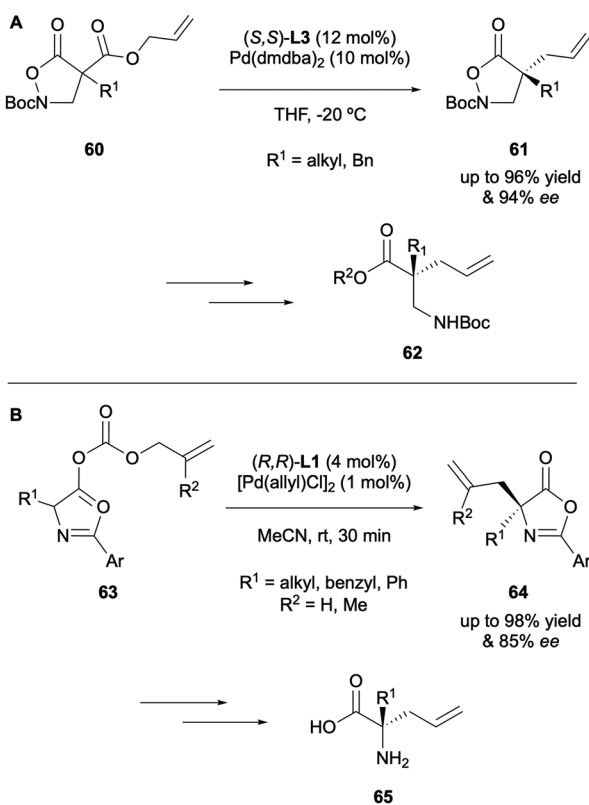
Scheme 16 DAAA of  $\alpha$ -enaminones by Stoltz.

Fig. 1 N,N-heterocycles by Stoltz

94% ee. The products of catalysis were then applied as precursors in the synthesis of enantioenriched  $\beta^{2,2}$ -amino acids **62** (Scheme 17A).<sup>32</sup> In 2019 Colombo described the DAAA of



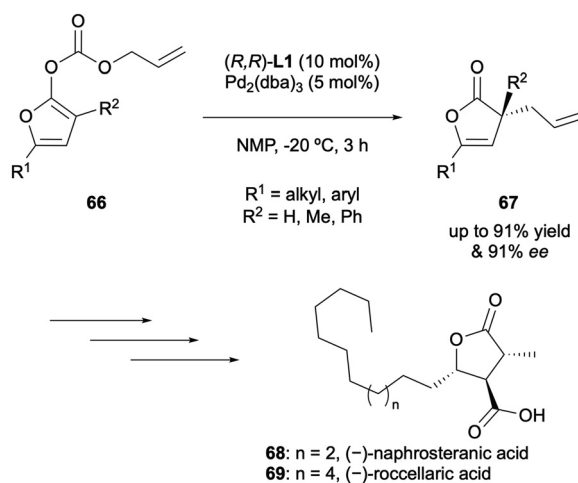
Scheme 17 DAAA of N,O-heterocycles by Shibasaki and Colombo.

azlactone enol carbonates **63** to generate precursors to quaternary  $\alpha$ -allyl amino acids **65**, in moderate enantioselectivities of up to 85% ee with (*R,R*)-DACH-phenyl Trost **L1** (Scheme 17B).<sup>33</sup> It was observed that substitution on the allyl fragment did not support high levels of asymmetric induction (30% ee when R<sub>2</sub> = Me), hence only compounds possessing an unsubstituted  $\alpha$ -allyl group were applied to the ring-opening reactions.

Oxygen-, sulfur- and silicon-containing heterocycles have not been as well explored in the DAAA catalysis, although the literature does contain several examples on the development of the reaction to support these motifs.

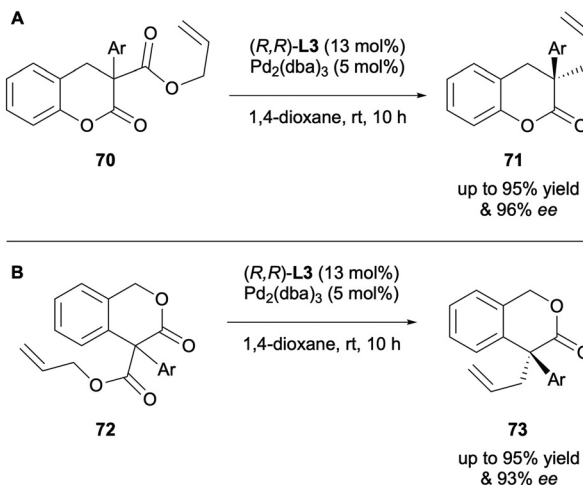
In 2013, Cossy and Arseniyadis described the DAAA of cyclic dienol carbonates **66** as a route to unsaturated quaternary stereocentres in butenolides with high levels of enantioselectivity of up to 91% ee (Scheme 18).<sup>34</sup> The nature of the substrates meant that the formation of both the  $\alpha$ -allylation and  $\gamma$ -allylation products was possible but system optimisation enabled up to 15 : 1 rr ( $\alpha$  :  $\gamma$ ). Both  $\alpha$ -alkyl and  $\alpha$ -aryl substituents were tolerated with (*R,R*)-DACH phenyl Trost **L1**. The synthetic utility of the generated products was demonstrated by performing a microwave-assisted Cope rearrangement to access the corresponding  $\gamma$ -tertiary and  $\gamma$ -quaternary 2(5*H*)furanones, with no erosion in enantio purity, which could be applied as intermediate in the synthesis of two members of the paraconic acid family.

The enantioselective DAAA of  $\alpha$ -aryl- $\beta$ -oxo esters **70** and **72** was developed by Guiry in 2016.<sup>35</sup> The (*R,R*)-ANDEN-phenyl Trost ligand **L3** was employed to prepare a series of  $\alpha$ -aryl- $\alpha$ -allyl-dihydrocoumarins **71** (Scheme 19A) and 3-isochromanone products **73** (Scheme 19B) in excellent yields and enantioselectivities of up to 96% and 93% ee, respectively. A range of  $\alpha$ -aryl groups were successfully tolerated with the same trend being observed as with previous examples; high levels of asymmetric induction is linked with the presence of di-*ortho* substitution.



Scheme 18 DAAA of cyclic dienol carbonates by Cossy &amp; Arseniyadis.

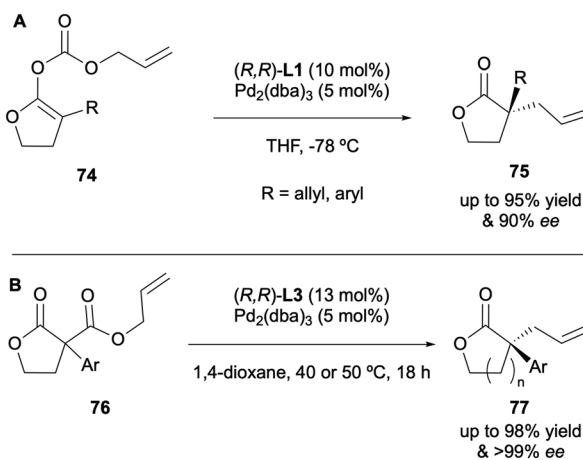
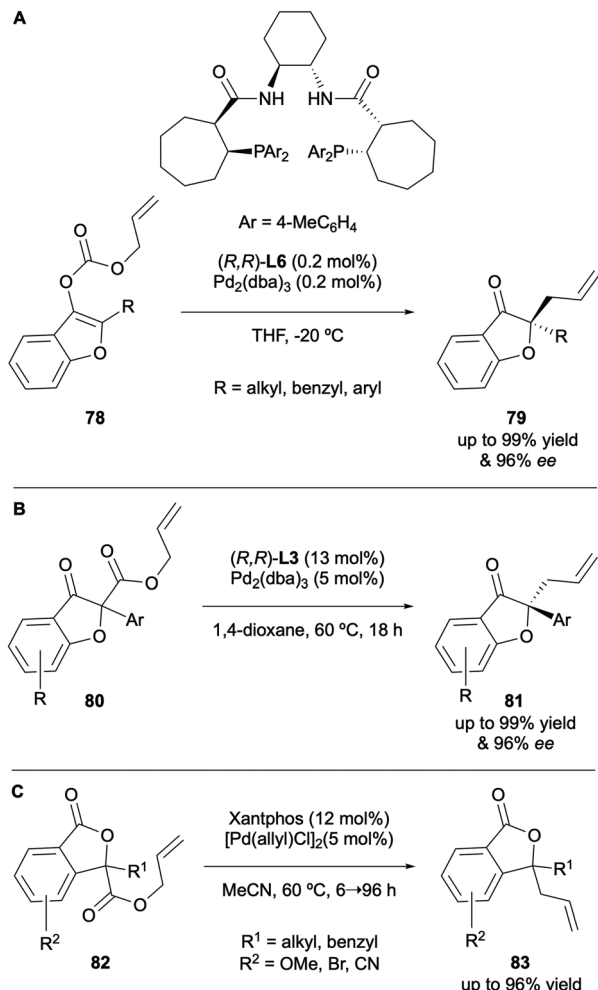




Scheme 19 DAAA of dihydrocoumarins and isochromanones by Guiry.

In 2017, Cossy and Arseniyadis further expanded on their previous work to include enol carbonates derived from  $\gamma$ -butyrolactones in the DAAA scope (Scheme 20A).<sup>36</sup> (*R,R*)-DACH phenyl Trost **L1** was the optimal ligand again, giving enantioselectivities of up to 90% ee. Enol carbonate substrates **74** derived from  $\alpha$ -acyl- $\gamma$ -butyrolactones were also successful under similar conditions, generating ee values of up to 94%. The same year Guiry and co-workers reported the highly enantioselective synthesis of  $\alpha$ -allyl- $\alpha$ -aryl five- and six-membered lactones *via* the DAAA protocol involving (*R,R*)-ANDEN-phenyl Trost **L3** to generate sterically hindered products with enantioselectivities of up to >99% (Scheme 20B).<sup>37</sup>

In 2020, Lu reported the DAAA of benzofuranone-derived enol carbonates **78** with novel Trost-type bisphosphane ligands which bear chiral cycloalkane frameworks (Scheme 21A).<sup>38</sup> The design and preparation of these saturated Trost-type ligands was required as the typical ligand systems used in DAAA did not afford high levels of enantioselectivity with these sub-

Scheme 20 Syntheses of  $\gamma$ -butyrolactones by Cossy & Arseniyadis and Guiry.

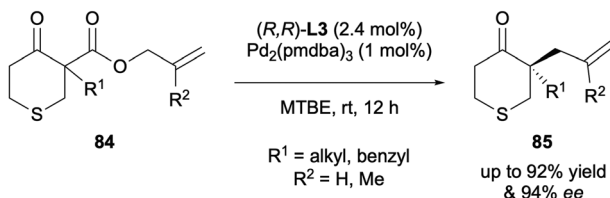
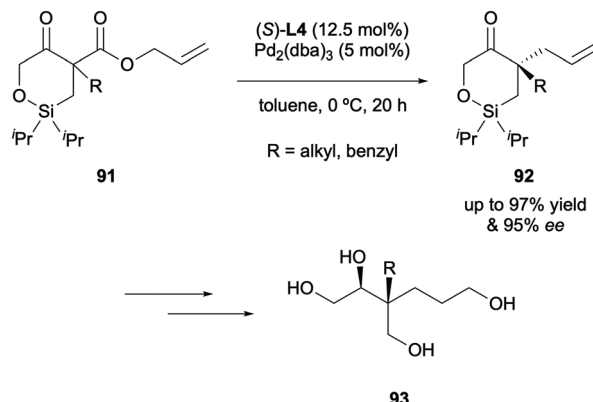
Scheme 21 DAAA of benzofuranones by Lu and Guiry.

strates. The system developed turned out to be highly efficient, requiring catalyst loadings of only 0.2–1 mol% to access the desired products in up to 96% ee.<sup>39</sup> In 2024, Guiry published the DAAA of  $\alpha$ -aryl benzofuranones in excellent enantioselectivities, of up to 96% ee with (*R,R*)-ANDEN-phenyl Trost **L3** (Scheme 21B).<sup>40</sup> The substrate scope included  $\alpha$ -allyl- $\alpha$ -aryl benzofuranones bearing substitution around the aromatic cyclic backbone. The decarboxylative allylic alkylation of phthalides was described by Navarro in 2022, employing the achiral ligand Xantphos in acetonitrile to access a range of products in yields of up to 96% (Scheme 21C).<sup>41</sup>

In 2017 the Stoltz group presented the DAAA of S-containing heterocycles, specifically  $\alpha$ -alkyl thiopyranones **84** (Scheme 22).<sup>42</sup> These  $\alpha$ -quaternary 4-thiopyranone products are challenging to access *via* standard enolate chemistry due to their potential for ring-opening through  $\beta$ -sulfur elimination. However, a range of substrates performed well in the catalysis, with (*R,R*)-ANDEN-phenyl Trost **L3** generating enantioselectivities of up to 94% ee.

Franckevičius and co-workers reported the synthesis of chiral thietane 1,1-dioxides **87** *via* DAAA with (*S,S*)-ANDEN-



Scheme 22 DAAA of  $\alpha$ -alkyl thiopyranones by Stoltz.

Scheme 24 DAAA of cyclic siloxyketones by Stoltz.

phenyl Trost **L3** in 2021 (Scheme 23A).<sup>43</sup> The highly enantio-enriched products of catalysis were employed as intermediates to access novel spirocycles with no enantioerosion observed. They published a second report the following year on the expansion of their methodology to include sulfolanes and thiane 1,1-dioxides **88** (Scheme 23B).<sup>44</sup> The scope also included thiomorpholine 1,1-dioxides. A key observation from both studies is the formation of an enantiomeric product despite the presence of an exocyclic enolate intermediate, as shown in Scheme 23C. This infers the occurrence of a Pd-mediated interconversion of the *E/Z* enolate intermediate prior to alkylation. It was demonstrated that the (*E*)-enolate is slower reacting than the (*Z*)-enolate, therefore a dynamic kinetic resolution is at play. From these results it can be said that as well as substituent sterics effecting asymmetric induction, so too does the rate of isomerisation of the enolate intermediate.

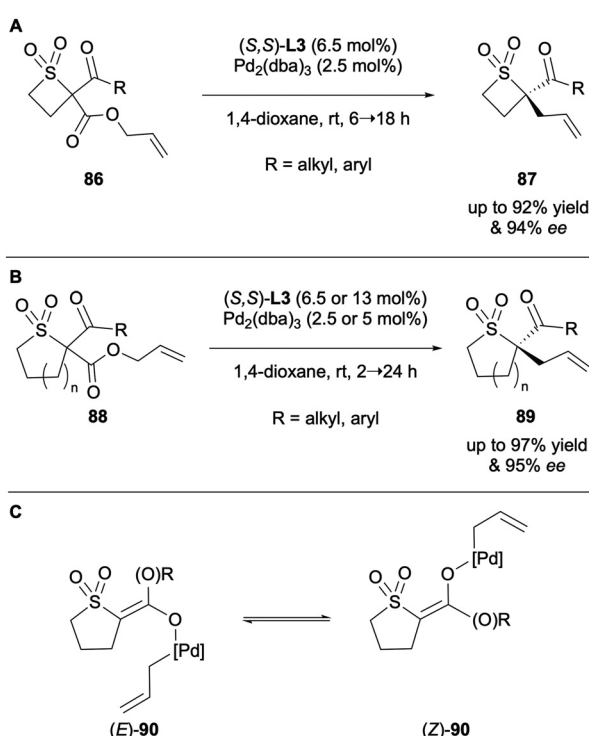
There is one example of siloxy- $\beta$ -keto allyl ester substrates being applied to the DAAA in the literature, reported by Stoltz in 2020 (Scheme 24).<sup>45</sup> Quaternary stereocentres were gener-

ated in high enantioselectivities of up to 94% ee with (*S*)-(CF<sub>3</sub>)<sub>3</sub>-*t*-Bu-PHOX **L4**. The significance of the products was highlighted in a ring-opening reaction to access highly oxygenated acyclic chiral compounds **93**.

Though less common, there are a handful of recent reports on the DAAA of acyclic substrates in the literature. These examples generally rely on a certain degree of steric bulk present to induce appreciable levels of asymmetric induction.

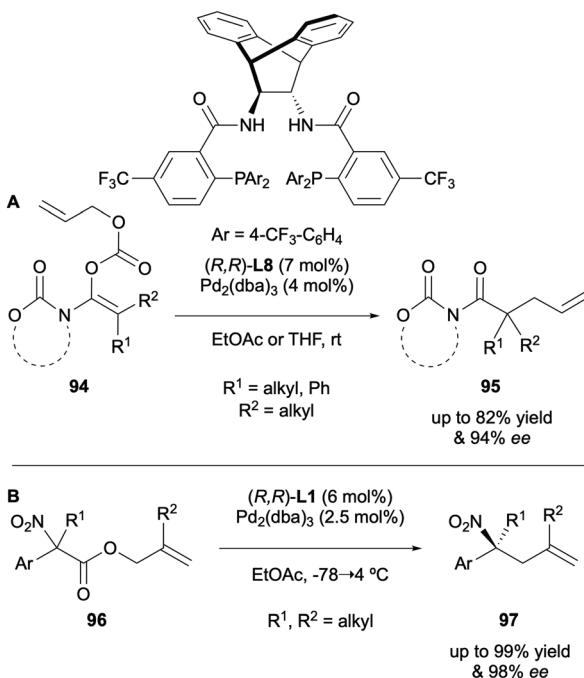
A range of acyclic amides **95** were synthesised through DAAA by Stoltz and Marek in 2017, utilising an electron-deficient Trost-type ligand to generate enantioselectivities of up to 94% ee (Scheme 25A).<sup>46</sup> A number of products were only isolated in moderate yields, which was attributed to undesired side reactions, such as  $\beta$ -hydride elimination and enolate protonation, or steric congestion. The DAAA of  $\alpha$ -nitroesters **96** was carried out by Trost in 2019 in order to employ the chiral products in the synthesis of the corresponding  $\alpha$ -tertiary nitroalkanes **97** (Scheme 25B).<sup>47</sup> A high dependency on solvent was observed, and by using (*R,R*)-DACH-phenyl Trost **L1** in ethyl acetate, the unwanted *O*-alkylation pathway was suppressed.

In 2020 Stoltz published the DAAA of benzoin-derived allyl enol carbonates **98** (Scheme 26A).<sup>48</sup> Unlike in previously discussed reports, the initial enolate geometry was found to be important to induce high levels of asymmetry. A reduction in *E/Z* ratio from 2 : 98 to 7 : 93 of the model substrate resulted in the enantiomeric excess decreasing by 13% ee. Hence, the substrates for catalysis had to be of high geometric purity to ensure high levels of enantioselectivity were achieved and implies that the dynamic effect observed by Franckevičius is not operating. In 2024, Ren and co-workers described the synthesis of chiral acyclic nitrile *via* an elegant synergistic DAAA and phase-transfer catalytic system from allyl 2-cyanoacetates **100** (Scheme 26B).<sup>49</sup> The approach offers a mild and efficient route to highly enantioenriched nitrile products, achieved with a sterically bulky achiral phosphane ligand and a chiral phase-transfer catalyst. This is distinct from all other approaches discussed, as the chirality is translated from the ionic species, not from the Pd complex.

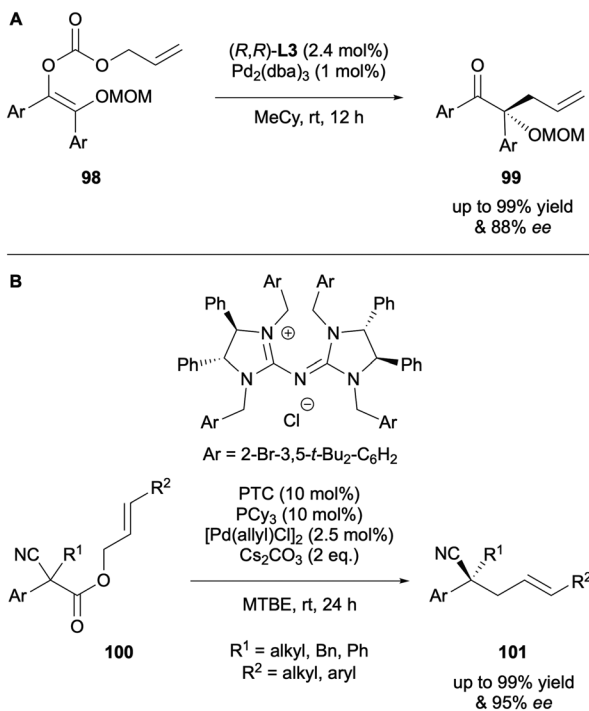


Scheme 23 DAAA of cyclic sulfones by Franckevičius.





Scheme 25 DAAA of acyclic amides and nitroesters.



Scheme 26 DAAA of benzoin derivatives and acyclic nitriles.

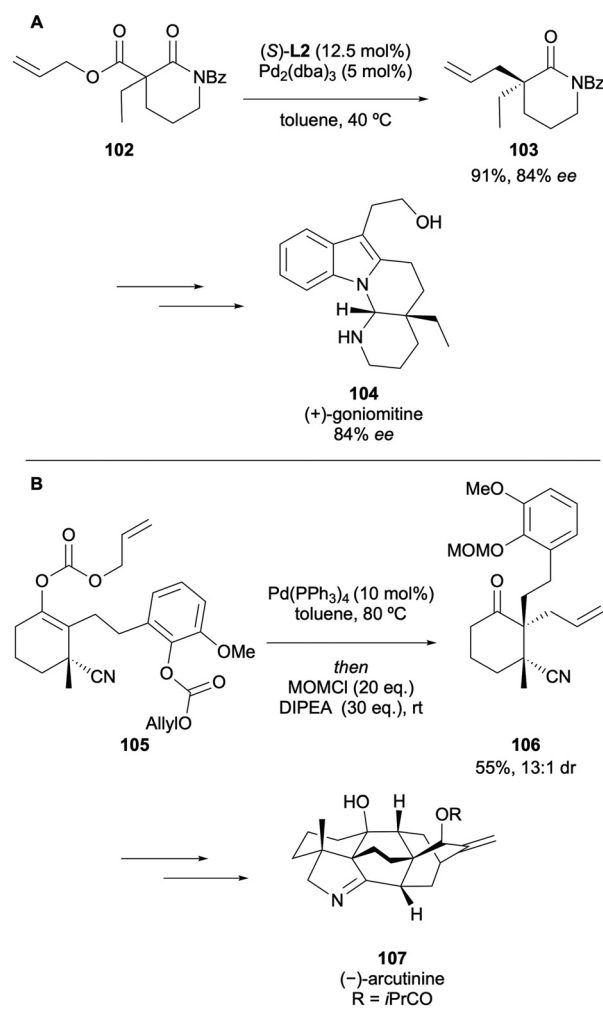
### Selected recent applications in natural product synthesis

The Pd-catalysed DAAA methodology has been employed as a key strategy to access intermediates in the syntheses of many all-carbon quaternary stereocentres present in natural products. Several total synthesis explorations have been under-

taken since the reaction was first reported. The selected examples discussed below will offer an overview of the most recent applications of the catalytic step in the synthesis of natural products.

In 2019, Cheon described the asymmetric total synthesis of (+)-goniomitine **104** in 84% ee from an ethyl 2-aminocinnamate and a chiral  $\alpha,\beta$ -unsaturated aldehyde that was accessed *via* the DAAA of  $\alpha$ -ethyl  $\beta$ -amido allyl ester **102** (Scheme 27A).<sup>50</sup> The Pd-catalysed DAAA step proceeded to generate the  $\delta$ -valerolactam **103** in an 84% ee, which demonstrates that the synthesis of (+)-goniomitine could be accomplished without any enantioerosion. A key intermediate **106** was accessed *via* the DAAA of allyl enol carbonate **105** for the enantioselective total synthesis of (–)-arcutinine **107**, reported by Qin in 2019 (Scheme 27B).<sup>51</sup> The chemistry was critical in setting the vicinal quaternary stereocentres at C4 and C5, enabling the first total synthesis of the C<sub>20</sub>-diterpenoid alkaloid.

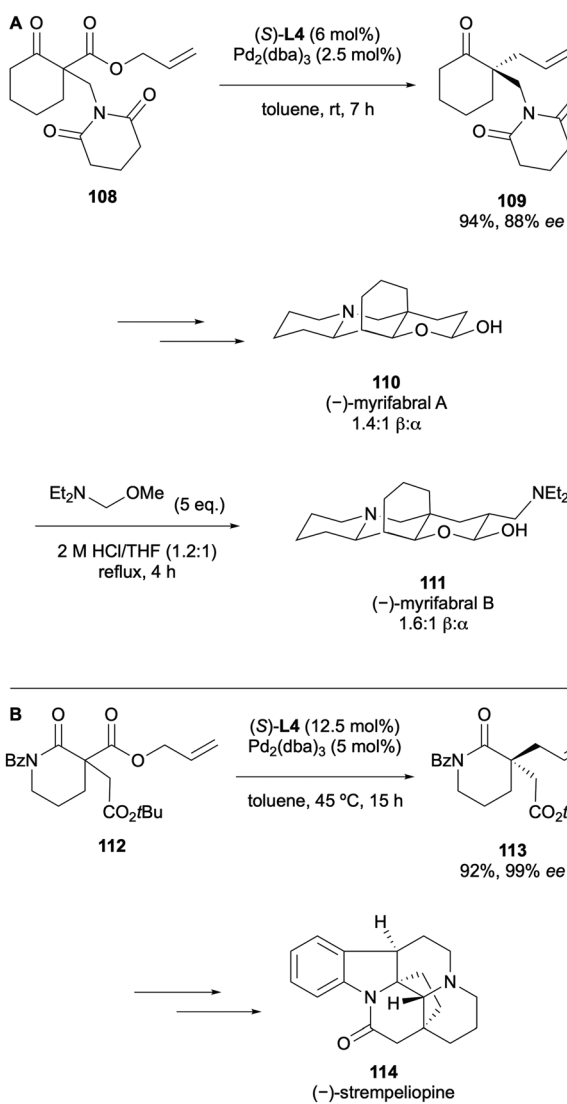
Stoltz published the first enantioselective total synthesis of (–)-myrifibral A and B in 2020.<sup>52</sup> The DAAA of cyclohexanone **108** was carried out on a 10 g scale to generate the corre-



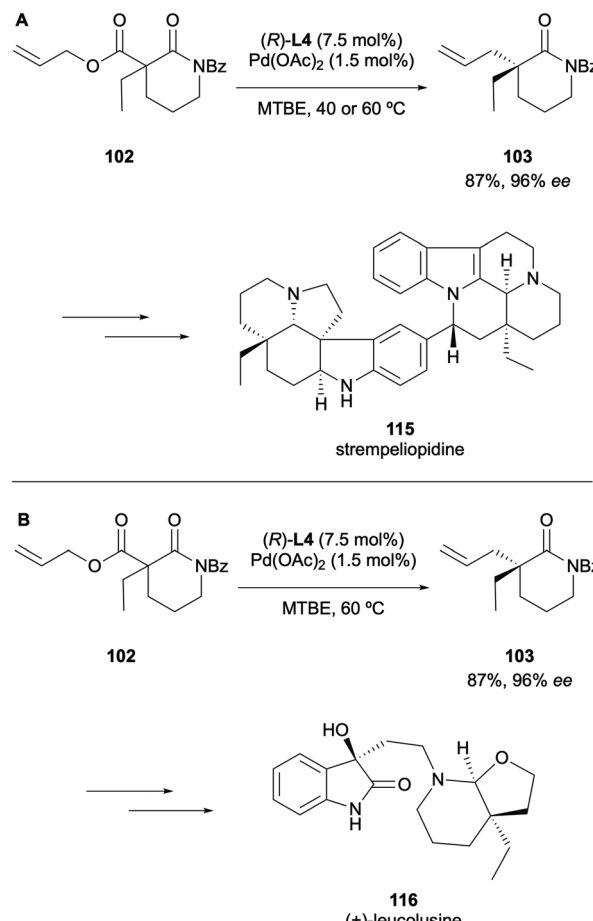
Scheme 27 DAAA in the syntheses of (+)-goniomitine and (–)-arcutinine.

ponding product in 88% ee using *(S)*-(CF<sub>3</sub>)<sub>3</sub>-*t*-BuPHOX **L4** (Scheme 28A). A further six steps generated *(–)*-myrifabral A, which provided access to *(–)*-myrifabral B *via* one additional transformation. The *(S)*-(CF<sub>3</sub>)<sub>3</sub>-*t*-BuPHOX ligand **L4** was very successful again in the total synthesis of *(–)*-strempeleiopine which was reported by Chen in 2022 (Scheme 28B).<sup>53</sup> The DAAA reaction produced the enantioenriched  $\alpha$ -quaternary lactam **113** in 99% ee. From this, a pentacyclic intermediate could be synthesised as a single diastereomer and hence, the *Schizozygine* alkaloid *(–)*-strempeleiopine **114** was accessed with high diastereoselectivity.

In 2023 Stoltz reported the total synthesis of strempeleiopine *via* a Pd-catalysed DAAA of lactam **102** (Scheme 29A).<sup>54</sup> The group synthesised eight stereoisomers of the bisindole alkaloid through a modular strategy. Most recently, in 2025, Chen described the total synthesis of *(+)*-leucolusine and *(–)*-7-



**Scheme 28** DAAA in the syntheses of *(–)*-myrifabral A and B and *(–)*-strempeleiopine.



**Scheme 29** DAAA in the syntheses of strempeleiopidine and *(+)*-leucolusine.

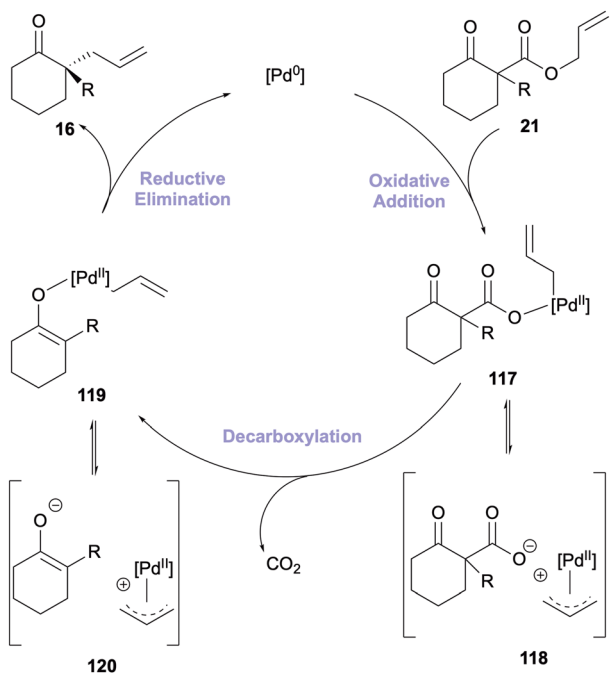
*epi*-leucolusine in eight steps.<sup>55</sup> The *cis*-fused octahydrofuro-[2,3- $\beta$ ]-pyridine intermediate was efficiently constructed through a one-pot methodology involving a reduction and an oxa-Mannich-type cyclisation of lactam **103**, which is generated *via* the same DAAA protocol that Stoltz applied for this substrate (Scheme 29B).

## Mechanism of the Pd-catalysed DAAA

The mechanism of the DAAA reaction is non-trivial, however the generalised cycle involves the Pd<sup>0</sup> complex coordinating to the allyl fragment which leads to oxidative addition of Pd into the C–O bond. This is followed by decarboxylation to generate the Pd-enolate ion-pair, after which the enolate goes on to attack the intermediate Pd- $\pi$ -allyl species. This reductive elimination step releases the enantioenriched product **16** and regenerates the Pd<sup>0</sup> catalyst (Scheme 30).<sup>14,56,57</sup>

Mechanistic studies have presented a more complex picture of the catalytic cycle, with the focus being mainly on systems employing Trost-type P,P and PHOX-type P,N ligands. Other factors such as solvent, substrate class and substitution patterns can also influence the mechanistic pathway





Scheme 30 Proposed general mechanism of the DAAA reaction.

undertaken.<sup>58–61</sup> This section aims to provide a concise discussion of the mechanistic investigations on the Pd-catalysed DAAA to date and hence, will be limited to those reactions employing Trost and PHOX ligands.

The initial step of the cycle has been generally accepted to involve a Pd-promoted ionisation of the ester or carbonate group, similar to the Tsuji–Trost reaction. The resulting Pd-carboxylate  $\pi$ -allyl ion pair **118** is most likely in equilibrium with the neutral  $\sigma$ -allyl complex **117**. Decarboxylation then occurs, which is a critical step in the formation of the enolate nucleophile. It is considered to be the rate limiting step of the mechanism. Two possible routes are postulated for decarboxylation, differing on whether Pd coordinates to the carbonyl oxygen after ionisation.<sup>62–64</sup>

The most contentious topic in understanding the DAAA mechanism is how the enantiodetermining reductive elimination proceeds, with two pathways proposed: an inner sphere and outer sphere mechanism (Fig. 2).

In 2007, DFT studies carried out by Stoltz and Goddard supported the inner sphere mechanism being favoured with PHOX-type P,N ligands.

The four-coordinate Pd complex is involved in a concerted process to generate the DAAA product *via* a seven-membered transition state.<sup>58</sup> This is lower in energy than the outer sphere pathway, which involves the nucleophilic enolate combining with the allyl species and eliminating the Pd complex. Subsequent mechanistic studies were performed on this Pd-PHOX system, namely deuterium labelling crossover experiments.<sup>65,66</sup> It was also observed that the system is tolerant of exogenous water, with both yields and enantioselectivities being maintained, inferring an inner sphere mechanism.

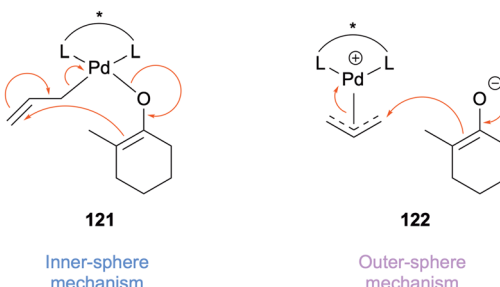


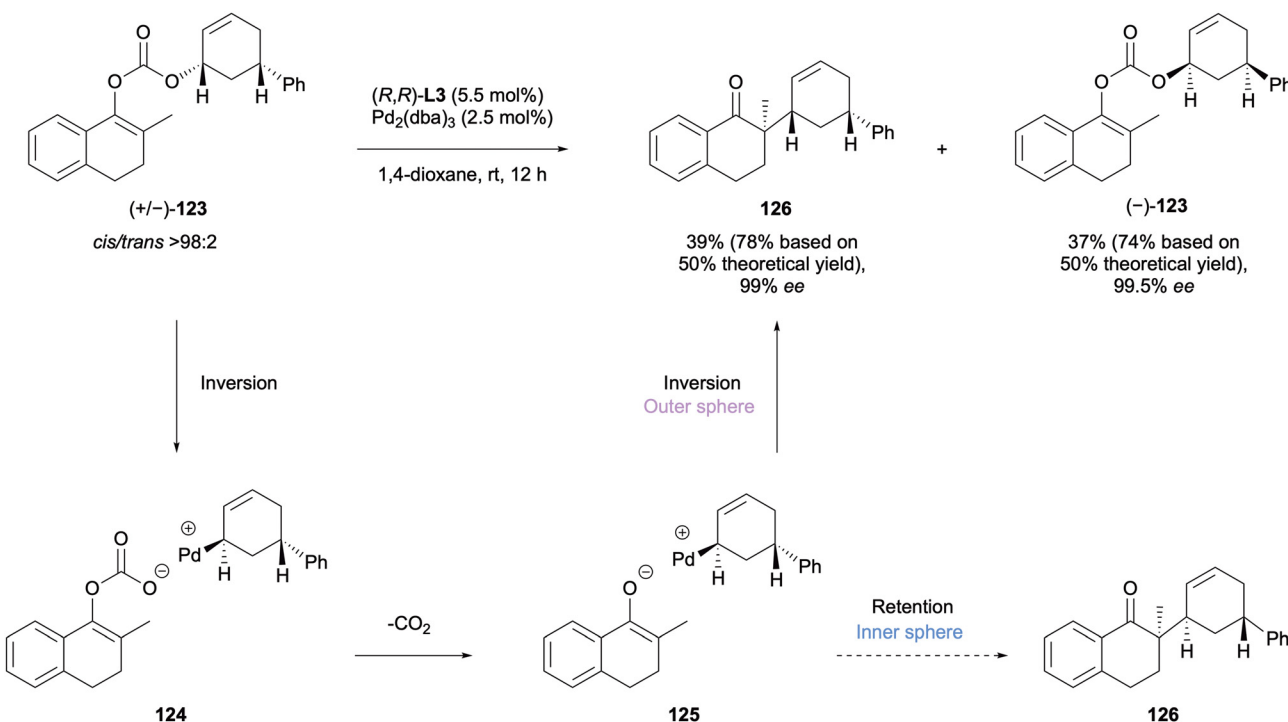
Fig. 2 Inner vs. outer sphere pathways.

Trost performed a mechanistic investigation of the DAAA protocol of enol carbonates employing the Trost ligands in 2009.<sup>57</sup> To determine what pathway was being undertaken in their system stereochemical probes were applied. Substrate **123** was subjected to the reaction conditions as a racemate and a kinetic resolution occurred to give one diastereomeric product in 99% ee with the other starting enantiomer remaining unreacted after 12 h (Scheme 31). The DAAA product formed displayed *cis* relative stereochemistry. This is a net stereoretention which is said to occur through a double inversion, supporting an outer sphere mechanism. The inner sphere mechanism would have been expected to generate the *trans*-diastereomer *via* a net inversion of the stereochemistry.

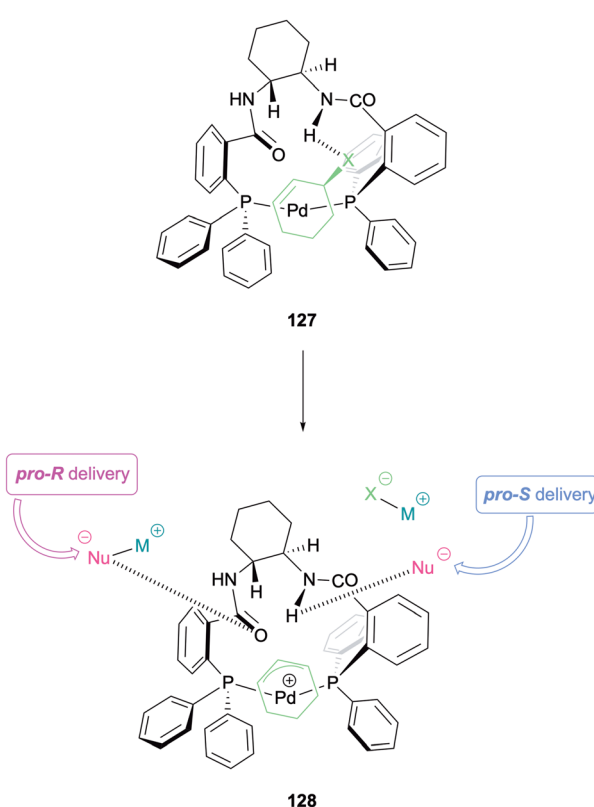
Later that same year Lloyd-Jones and Norrby reported their mechanistic work on the AAA reaction with Trost-type ligands, further solidifying support for an outer sphere mechanism with this system.<sup>59</sup> Exploiting a combination of NMR spectroscopy, isotopic labelling, and computational investigations monomeric Pd- $\eta^3$ -allyl and Pd- $\eta^3$ -cyclohexenyl complexes with (*R,R*)-DACH-phenyl Trost were elucidated (Scheme 32). A 13-membered chelate was formed, producing a concave species **128**. *Pro-S* delivery arises from H-bonding between the nucleophilic enolate and the amide that has its N-H projecting forward towards one of the allyl termini. *Pro-R* delivery would have to be assisted by an escort ion ( $M^+$ ), which strongly coordinates to the carbonyl of the opposite amide, projecting out of the complex, weakening the H-bonding of the other amide. This study concluded that the mechanism is outer sphere with respect to the Pd centre and inner sphere for the Pd- $\pi$ -allyl-ligand complex.

In 2012 Stoltz and Goddard further extended their investigations into the reductive elimination step of the reaction with the PHOX ligand system.<sup>60</sup> Three separate computational pathways with varying level of theory supported the lower energy inner sphere mechanism being favoured. None of the DFT calculations for the outer sphere pathway correlated with the observed stereoselectivities. Continuing with the ideas suggested in their 2007 report, the authors proposed that the five-coordinate complex **129** undergoes an internal rearrangement to the four-coordinate complex **131** *via* transition state **130** (Scheme 33), which was calculated as the key enantiodetermining step based on the energy difference between the *Re*- and *Si*-pathways. Reductive elimination then occurs unconventionally, through the seven-membered transition state, as pre-





Scheme 31 Mechanistic investigations with Trost ligands.



Scheme 32 Model for nucleophile delivery by Lloyd-Jones and Norrby.

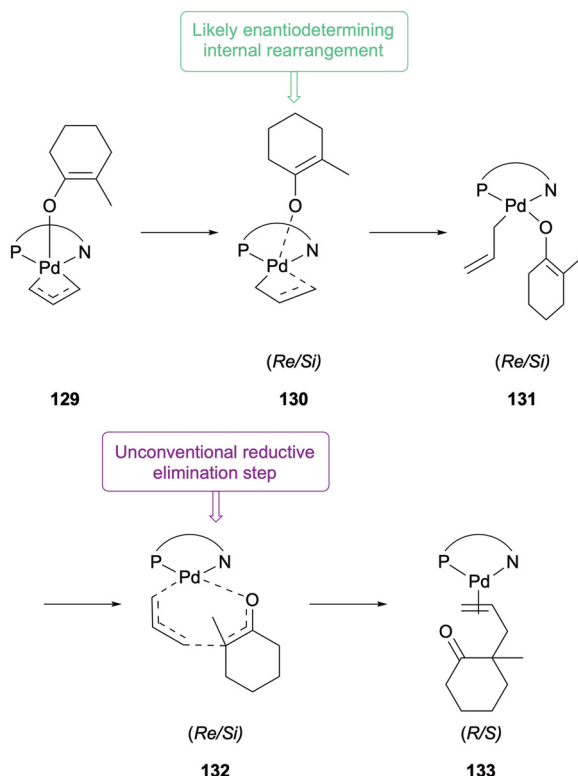
viously proposed, to generate the DAAA product before ligand dissociation and catalyst regeneration.

Stoltz and Goddard published a comprehensive quantum mechanical evaluation of the entire DAAA catalytic cycle with  $\beta$ -keto allyl ester substrates in 2020 (Scheme 34).<sup>61</sup> The report united all their experimental findings of the inner sphere mechanism to design the computational framework. The DFT study confirmed that the enantiodetermining step for the inner sphere mechanism is the formation of the C(sp<sup>3</sup>)-C(sp<sup>3</sup>) bond *via* the seven-coordinate transition state, rather than in the rearrangement as previously proposed (Scheme 34). Additionally, it was noted that the inner sphere pathway is favoured when solvent polarity decreases as the ionic intermediates of the outer-sphere mechanism are destabilised and that degradation of enantiocontrol is observed in the energetically unfavourable outer sphere process.

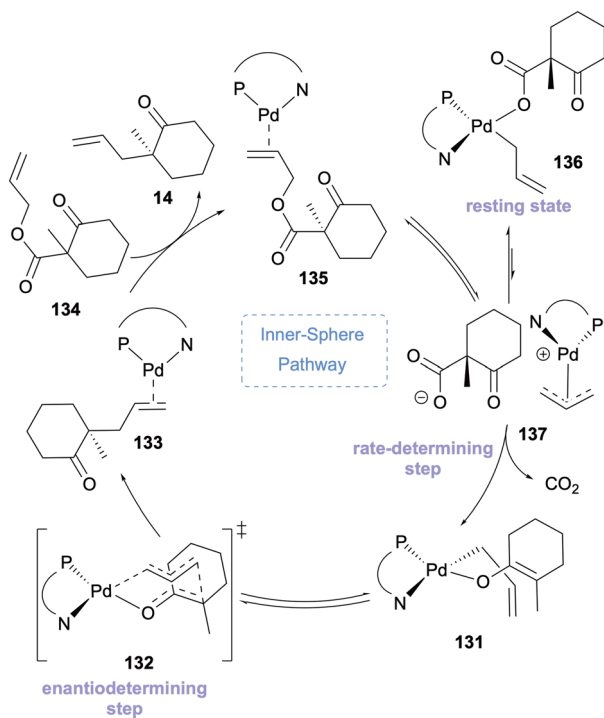
In 2023 Arseniyadis and Leitch described the preparation of bench stable chiral Pd0 precatalysts for use in allylic alkylations.<sup>67</sup> Within the library of complexes synthesised, Trost-type and PHOX-type ligands were incorporated. Full characterisation, including X-Ray diffraction analysis, allowed elucidation of solution and solid-state conformations. Importantly, study of the precatalyst (S,S)-<sup>NAP</sup>DACH-Pd-MAH showed the intramolecular hydrogen bond between the N-H of one of the ligand amides and the carbonyl of the coordinating maleic anhydride (Fig. 3), as originally proposed by Lloyd-Jones and Norrby.<sup>59</sup>

Stoltz, Goddard and co-workers also published a study in 2023, exploring why N-benzoyl lactams display enhanced enantioselectivity in the Pd-catalysed DAAA compared to their





Scheme 33 Transition state model with PHOX-type ligands.



Scheme 34 Updated inner-sphere mechanism.

carbocycle counterparts.<sup>68</sup> They had observed that enantioenrichment of  $\alpha$ -alkyl carbocyclic products is limited to 80–90% ee whereas enantioselectivities of >99% ee can be accessed

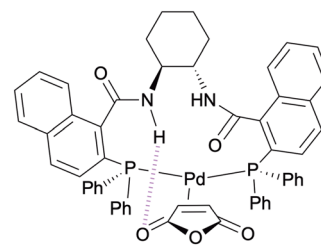
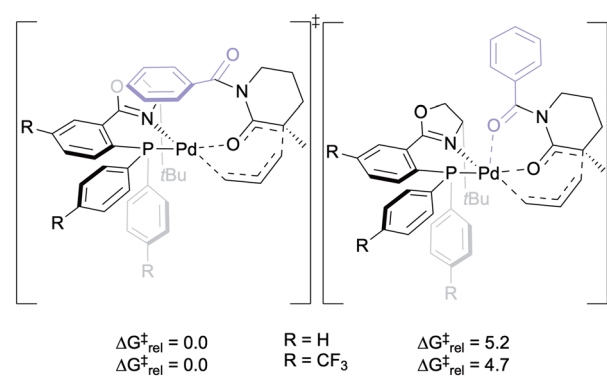


Fig. 3 Pre-catalyst complex coordination with maleic anhydride.

with *N*-benzoyl lactams.<sup>10,22</sup> The group employed DFT calculations to help interpret their experimental findings and from this proposed that this enhanced enantioselectivity is due to noncovalent interactions between the substrate and the ligand and not secondary substrate chelation which was previously thought to be the case. The axial Pd–O distances calculated do not support a strong interaction and it was found that the four-coordinate TS is the more energetically favourable conformation (Fig. 4). The benzoyl group orients to be parallel to the open face of the PHOX ligand backbone. The lower enantioselectivities observed for *N*-carbamate groups, such as Boc, CBz and Fmoc, were explained to be as a result of these protecting groups being more Lewis basic.

In addition to using computational studies like DFT as a valuable tool to deepen our understanding of the DAAA mechanism, the emergence and rapid growth of machine learning (ML) applications in chemistry has inspired the consideration that substrate performance in the DAAA catalysis could be predicted prior to experimental investigation. In 2025 Reid and co-workers published a report on a data-driven method to predict models of enantioinduction in asymmetric catalytic reactions.<sup>69</sup> Using the Pd-catalysed DAAA reaction as their model, the developed ML approach highlighted enantioselectivity is influenced by solvent to a greater degree than previously thought. Their method elegantly simplifies the challenge of mechanistic generalisation to make it more accurate.

In conclusion, the intricacies of the mechanism of DAAA have been well investigated since the initial report of the reaction. A general mechanistic pathway has been outlined, and

Fig. 4 DFT calculated transition states of the *N*-benzoyl lactam substrates.

particular attention has been placed on deepening understanding of the key enantiodetermining reductive elimination step. Discussions on whether the inner sphere or outer sphere pathway is at play has led to strong evidence supporting that both can, and do, occur and that the mechanism undertaken is dependent on the ligand system employed, but ultimately a range of factors have to be considered in the design of an optimal system for catalysis with various substrates.

## Conclusions

This review outlined the origins of Pd-catalysed decarboxylative allylic alkylation, followed by the asymmetric variant and its development, including more recent examples. Selected applications of this asymmetric protocol to natural product synthesis have also been given. Finally, a concise description of the mechanistic studies performed to date, including labelling, spectroscopic and computational studies, is detailed. While studies have extensively explored mechanistic understanding, there has not been much focus on adapting the methodology for industrial application, which would increase the usefulness of the chemistry. Preliminary work has commenced in employing ML as an approach to predict enantioinduction in the DAAA reaction and the field is growing. The aim of these efforts would be to use the results to inform what reactions conditions are more likely to be successful, hence reducing the time spent, and materials used, screening conditions experimentally.

## Conflicts of interest

There are no conflicts to declare.

## Data availability

No primary research results, software or code have been included and no new data were generated or analysed as part of this review.

## Acknowledgements

N. L. acknowledges the financial support for her PhD scholarship from Atoms 2 Products CDT supported by Research Ireland and the Engineering and Physical Sciences Research Council (EPSRC) under Grant No. 18/EPSRC-CDT/3582. BiOrbic is funded by Ireland's European Structural and Investment Programmes, Science Foundation Ireland (16/RC/3889) and the European Regional Development Fund.

## References

- 1 M. Carroll, *J. Am. Chem. Soc.*, 1940, **70**, 704–706.
- 2 A. M. Martín Castro, *Chem. Rev.*, 2004, **104**, 2939–3002.
- 3 H. Pommer and A. Nürrenbach, in *Organic Synthesis*, Elsevier, 1975, pp. 527–551.
- 4 J. Tsuji and T. Susuki, *Tetrahedron Lett.*, 1965, **6**, 3027–3031.
- 5 B. M. Trost and T. J. Fullerton, *J. Am. Chem. Soc.*, 1973, **95**, 292–294.
- 6 B. M. Trost and P. E. Strege, *J. Am. Chem. Soc.*, 1977, **99**, 1649–1651.
- 7 I. Shimizu, T. Yamada and J. Tsuji, *Tetrahedron Lett.*, 1980, **21**, 3199–3202.
- 8 T. Tsuda, Y. Chujo, S. Nishi, K. Tawara and T. Saegusa, *J. Am. Chem. Soc.*, 1980, **102**, 6381–6384.
- 9 E. C. Burger and J. A. Tunge, *Org. Lett.*, 2004, **6**, 4113–4115.
- 10 D. C. Behenna and B. M. Stoltz, *J. Am. Chem. Soc.*, 2004, **126**, 15044–15045.
- 11 B. M. Trost and J. Xu, *J. Am. Chem. Soc.*, 2005, **127**, 2846–2847.
- 12 B. M. Trost and J. Xu, *J. Am. Chem. Soc.*, 2005, **127**, 17180–17181.
- 13 J. T. Mohr, D. C. Behenna, A. M. Harned and B. M. Stoltz, *Angew. Chem., Int. Ed.*, 2005, **44**, 7084–7087.
- 14 J. James, M. Jackson and P. J. Guiry, *Adv. Synth. Catal.*, 2019, **361**, 3016–3049.
- 15 X. Yu, T. Zhang, J. Liu and X. Li, *Synthesis*, 2021, **53**, 4341–4352.
- 16 C. M. Reeves, C. Eidamshaus, J. Kim and B. M. Stoltz, *Angew. Chem., Int. Ed.*, 2013, **52**, 6718–6721.
- 17 R. A. Craig, S. A. Loskot, J. T. Mohr, D. C. Behenna, A. M. Harned and B. M. Stoltz, *Org. Lett.*, 2015, **17**, 5160–5163.
- 18 R. Akula, R. Doran and P. J. Guiry, *Eur. J. Chem.*, 2016, **22**, 9938–9942.
- 19 C. Kingston, F. B. Meany, Y. Ortin and P. J. Guiry, *Tetrahedron*, 2025, **183**, 134713.
- 20 L. Fliegel, M. Schmidmann and J. Christoffers, *Org. Lett.*, 2024, **26**, 10600–10603.
- 21 E. Vitaku, D. T. Smith and J. T. Njardarson, *J. Med. Chem.*, 2014, **57**, 10257–10274.
- 22 D. C. Behenna, Y. Liu, T. Yurino, J. Kim, D. E. White, S. C. Virgil and B. M. Stoltz, *Nat. Chem.*, 2012, **4**, 130–133.
- 23 B. M. Trost, A. Nagaraju, F. Wang, Z. Zuo, J. Xu and K. L. Hull, *Org. Lett.*, 2019, **21**, 1784–1788.
- 24 D. J. Galvin and P. J. Guiry, *Eur. J. Org. Chem.*, 2024, e202400314.
- 25 V. Franckevicius, J. D. Cuthbertson, M. Pickworth, D. S. Pugh and R. J. Taylor, *Org. Lett.*, 2011, **13**, 4264–4267.
- 26 M. Jackson, C. Q. O'Broin, H. Müller-Bunz and P. J. Guiry, *Org. Biomol. Chem.*, 2017, **15**, 8166–8178.
- 27 K. M. Korch, C. Eidamshaus, D. C. Behenna, S. Nam, D. Horne and B. M. Stoltz, *Angew. Chem., Int. Ed.*, 2015, **54**, 179–183.
- 28 D. C. Duquette, A. Q. Cusumano, L. Lefoulon, J. T. Moore and B. M. Stoltz, *Org. Lett.*, 2020, **22**, 4966–4969.
- 29 N. B. Bennett, D. C. Duquette, J. Kim, W. B. Liu, A. N. Marziale, D. C. Behenna, S. C. Virgil and B. M. Stoltz, *Chem. – Eur. J.*, 2013, **19**, 4414–4418.



30 Z. P. Sercel, A. W. Sun and B. M. Stoltz, *Org. Lett.*, 2019, **21**, 9158–9161.

31 Z. P. Sercel, A. W. Sun and B. M. Stoltz, *Org. Lett.*, 2021, **23**, 6348–6351.

32 J. S. Yu, H. Noda and M. Shibasaki, *Angew. Chem.*, 2018, **130**, 826–830.

33 M. Serra, E. Bernardi, G. Marrubini, E. De Lorenzi and L. Colombo, *Eur. J. Org. Chem.*, 2019, 732–741.

34 J. Fournier, O. Lozano, C. Menozzi, S. Arseniyadis and J. Cossy, *Angew. Chem.*, 2013, **125**, 1295–1299.

35 R. Akula and P. J. Guiry, *Org. Lett.*, 2016, **18**, 5472–5475.

36 M. Nascimento de Oliveira, J. Fournier, S. Arseniyadis and J. Cossy, *Org. Lett.*, 2017, **19**, 14–17.

37 J. James and P. J. Guiry, *ACS Catal.*, 2017, **7**, 1397–1402.

38 M.-Y. Cao, B.-J. Ma, Z.-Q. Lao, H. Wang, J. Wang, J. Liu, K. Xing, Y.-H. Huang, K.-J. Gan, W. Gao, H. Wang, X. Hong and H.-H. Lu, *J. Am. Chem. Soc.*, 2020, **142**, 12039–12045.

39 H.-H. Lu and M.-Y. Cao, *Synlett*, 2021, **32**, 1981–1986.

40 F. McNeill, B. Twamley and P. J. Guiry, *Chem. – Eur. J.*, 2024, **30**, e202401738.

41 T. J. McClure, C. Saludares, G. Martinez, C. Orozco and R. Navarro, *J. Org. Chem.*, 2022, **87**, 7557–7564.

42 E. J. Alexy, S. C. Virgil, M. D. Bartberger and B. M. Stoltz, *Org. Lett.*, 2017, **19**, 5007–5009.

43 G. Laidlaw and V. Franckevičius, *Org. Lett.*, 2021, **24**, 400–405.

44 E. Bowen, G. Laidlaw, B. C. Atkinson, T. A. McArdle-Ismaguilov and V. Franckevicius, *J. Org. Chem.*, 2022, **87**, 10256–10276.

45 A. Ngamnithiporn, T. Iwayama, M. D. Bartberger and B. M. Stoltz, *Chem. Sci.*, 2020, **11**, 11068–11071.

46 P. Starkov, J. T. Moore, D. C. Duquette, B. M. Stoltz and I. Marek, *J. Am. Chem. Soc.*, 2017, **139**, 9615–9620.

47 B. M. Trost, J. E. Schultz and Y. Bai, *Angew. Chem., Int. Ed.*, 2019, **58**, 11820–11825.

48 R. Lavernhe, E. J. Alexy, H. Zhang and B. M. Stoltz, *Adv. Synth. Catal.*, 2020, **362**, 344–347.

49 C. Guo, Y. Dong, Y. Wang, X. Du, R. Ma, C.-H. Tan, X. Luan and J. Ren, *ACS Catal.*, 2024, **14**, 18841–18850.

50 E. Park and C.-H. Cheon, *Adv. Synth. Catal.*, 2019, **361**, 4888–4892.

51 W. Nie, J. Gong, Z. Chen, J. Liu, D. Tian, H. Song, X.-Y. Liu and Y. Qin, *J. Am. Chem. Soc.*, 2019, **141**, 9712–9718.

52 T. J. Fulton, A. Y. Chen, M. D. Bartberger and B. M. Stoltz, *Chem. Sci.*, 2020, **11**, 10802–10806.

53 Y. An, M. Wu, W. Li, Y. Li, Z. Wang, Y. Xue, P. Tang and F. Chen, *Chem. Commun.*, 2022, **58**, 1402–1405.

54 A. W. Rand, K. J. Gonzalez, C. E. Reimann, S. C. Virgil and B. M. Stoltz, *J. Am. Chem. Soc.*, 2023, **145**, 7278–7287.

55 H. Chen, Y. Li, L. Yu, X. Hu, H. Wang, Q. Wang, P. Tang and F.-E. Chen, *Org. Lett.*, 2025, **27**, 4992–4996.

56 O. Pàmies, J. Margalef, S. Cañellas, J. James, E. Judge, P. J. Guiry, C. Moberg, J.-E. Backvall, A. Pfaltz and M. A. Pericàs, *Chem. Rev.*, 2021, **121**, 4373–4505.

57 B. M. Trost, J. Xu and T. Schmidt, *J. Am. Chem. Soc.*, 2009, **131**, 18343–18357.

58 J. A. Keith, D. C. Behenna, J. T. Mohr, S. Ma, S. C. Marinescu, J. Oxgaard, B. M. Stoltz and W. A. Goddard, *J. Am. Chem. Soc.*, 2007, **129**, 11876–11877.

59 C. P. Butts, E. Filali, G. C. Lloyd-Jones, P.-O. Norrby, D. A. Sale and Y. Schramm, *J. Am. Chem. Soc.*, 2009, **131**, 9945–9957.

60 J. A. Keith, D. C. Behenna, N. Sherden, J. T. Mohr, S. Ma, S. C. Marinescu, R. J. Nielsen, J. Oxgaard, B. M. Stoltz and W. A. Goddard III, *J. Am. Chem. Soc.*, 2012, **134**, 19050–19060.

61 A. Q. Cusumano, B. M. Stoltz and W. A. Goddard III, *J. Am. Chem. Soc.*, 2020, **142**, 13917–13933.

62 J. V. Rund and R. A. Plane, *J. Am. Chem. Soc.*, 1964, **86**, 367–371.

63 D. J. Dahrenbourg, M. W. Holtcamp, B. Khandelwal, K. K. Klausmeyer and J. H. Reibenspies, *Inorg. Chem.*, 1995, **34**, 2389–2398.

64 D. Imao, A. Itoi, A. Yamazaki, M. Shirakura, R. Ohtoshi, K. Ogata, Y. Ohmori, T. Ohta and Y. Ito, *J. Org. Chem.*, 2007, **72**, 1652–1658.

65 N. H. Sherden, D. C. Behenna, S. C. Virgil and B. M. Stoltz, *Angew. Chem., Int. Ed.*, 2009, **48**, 6840–6843.

66 D. C. Behenna, J. T. Mohr, N. H. Sherden, S. C. Marinescu, A. M. Harned, K. Tani, M. Seto, S. Ma, Z. Novák and M. R. Krout, *Chem. – Eur. J.*, 2011, **17**, 14199–14223.

67 J. Huang, T. Keenan, F. Richard, J. Lu, S. E. Jenny, A. Jean, S. Arseniyadis and D. C. Leitch, *Nat. Commun.*, 2023, **14**, 8058.

68 A. Q. Cusumano, T. Zhang, W. A. Goddard III and B. M. Stoltz, *Catalysts*, 2023, **13**, 1258.

69 I. O. Betinol, Y. Kuang, J. Lai, C. Yousofi and J. P. Reid, *ACS Catal.*, 2025, **15**, 8799–8810.

